

The nature and origin of the carbonatite-hosted Wicheeda rare earth element deposit, British Columbia

Trofanenko, J.¹, Williams-Jones, A.E.^{1, a}, and Simandl, G.J.^{2, 3}

¹ McGill University, Department of Earth and Planetary Sciences, Montreal, QC, H3A 0E8

² British Columbia Geological Survey, Ministry of Energy and Mines, Victoria, BC, V8W 9N3

³ University of Victoria, School of Earth and Ocean Sciences, Victoria, BC, V8P 5C2

^a corresponding author: anthony.williams-jones@mcgill.ca

Recommended citation: Trofanenko, J., Williams-Jones, A.E., and Simandl, G.J., 2014. The nature and origin of the carbonatite-hosted Wicheeda Lake rare earth element deposit. In: Geological Fieldwork 2013, British Columbia Ministry of Energy and Mines, British Columbia Geological Survey Paper 2014-1, pp. 213-225.

Abstract

The Wicheeda rare earth element (REE) deposit is an example of high-grade REE mineralization in the British Columbia alkaline province. The deposit is hosted by a 145 m thick, steeply dipping lens-shaped carbonatite that intruded metasedimentary rocks of the Kechika Group, and is exposed over an area of ~ 20,000 m². The metasedimentary rocks comprise steeply dipping limestone and siltstone that were regionally metamorphosed to greenschist facies. These rocks were subjected to alkali metasomatism, which produced potassic fenite (K-feldspar- and biotite-rich) adjacent to the carbonatite and sodic fenite (sodic amphibole- and albite-rich) at a greater distance from it. Most of the REE mineralization is hosted by pervasively altered carbonatite, consisting of coarse-grained cream-coloured dolomite crystals rimmed by hematite, together with disseminated fine-grained biotite, pyrite, and trace apatite. The intrusion was affected by multi-stage dolomitization and fracture-associated dissolution of dolomite followed by precipitation of REE-bearing minerals (e.g., bastnäsite-(Ce) and monazite-(Ce)) along fractures and in vugs. Monazite-(Ce) occurs as fine-grained aggregates and rarely as lath-shaped inclusions in bastnäsite-(Ce), suggesting that it preceded bastnäsite-(Ce). The deposit is light-REE (LREE) enriched with a La/Lu ratio of 4314 in the dolomite carbonatite compared to 1249 in the potassic fenite and 46 in the sodic fenite. Total rare earth oxide concentrations in the deposit range from 1.1 to 11 wt.%. Cerium and lanthanum concentrations reach 5.3 and 4.1 wt.%, respectively. We propose a preliminary model in which a halogen- (mainly chlorine) and alkali-bearing hydrothermal fluid exsolved from the carbonatite magma, altered the adjacent sedimentary rocks to potassic fenite, and mobilized the REEs as chloride complexes. Distal to the intrusion, heating of formational waters by the carbonatite altered the sedimentary rocks to sodic fenite. The magmatic hydrothermal fluid partially dissolved the carbonatite, leading to deposition of bastnäsite-(Ce) and monazite-(Ce) in veins and vugs in response to an increase in pH. The Wicheeda carbonatite demonstrates the potential for economic carbonatite-hosted hydrothermal REE deposits in British Columbia.

Keywords: Wicheeda Lake, rare earth element deposit, carbonatite, fenitization, bastnäsite-(Ce), monazite-(Ce), hydrothermal concentration, REE-chloride complexes, fluid mixing

1. Introduction

The British Columbia alkaline province represents a potentially important but largely unexplored rare metal metallogenic province in the foreland fold and thrust belt of the Canadian Cordillera (Fig. 1 inset) that owes its origin to a change from convergent to extensional tectonics at ~ 390 Ma (Pell, 1994). This change in tectonics caused rifting that provided access for mantle-derived magmas to the crust, and led to the emplacement of a number carbonatite bodies between ~ 360 and 330 Ma (Pell, 1994; Millonig et al., 2012), including the Wicheeda intrusion, which hosts a high-grade REE deposit. The REE potential of the Wicheeda carbonatite, approximately 100 km northeast of Prince George in north-central British Columbia (Fig. 1), was first recognized by Mäder and Greenwood (1987), who described it as a 250 m diameter plug characterized by ankerite phenocrysts, unconfirmed REE-fluorocarbonates, and “baked sediments” including limestone interbedded with silty to shaley limestone, and shale of the Kechika Group (Cambrian to Early Ordovician; Betmanis,

1987). Subsequent exploration of the carbonatite by Spectrum Mining Corporation revealed a LREE-enriched deposit from drill intersections of carbonatite containing total rare earth concentrations (Σ REE) up to 3.4 wt.% REE (predominantly LREE), 0.4 wt.% niobium, and 0.2 wt.% molybdenum over 48.6 m (Lane 2009, 2010).

This study documents the nature of the Wicheeda carbonatite and its host rocks, provides a detailed description of the REE mineralization, and makes a preliminary interpretation of the genesis of this mineralization, based on detailed mapping of outcrops, diamond drill core logging, optical and EDS-assisted scanning electron microscopy, and bulk rock geochemical analyses. The principal findings of the study are: the carbonatite comprises a dolomitic core and a thin outer calcitic facies; bastnäsite-(Ce) and subordinate monazite-(Ce) are the main REE minerals; and the REE mineralization was the product of magmatic hydrothermal fluids, which also fenitized the surrounding metasedimentary rocks.

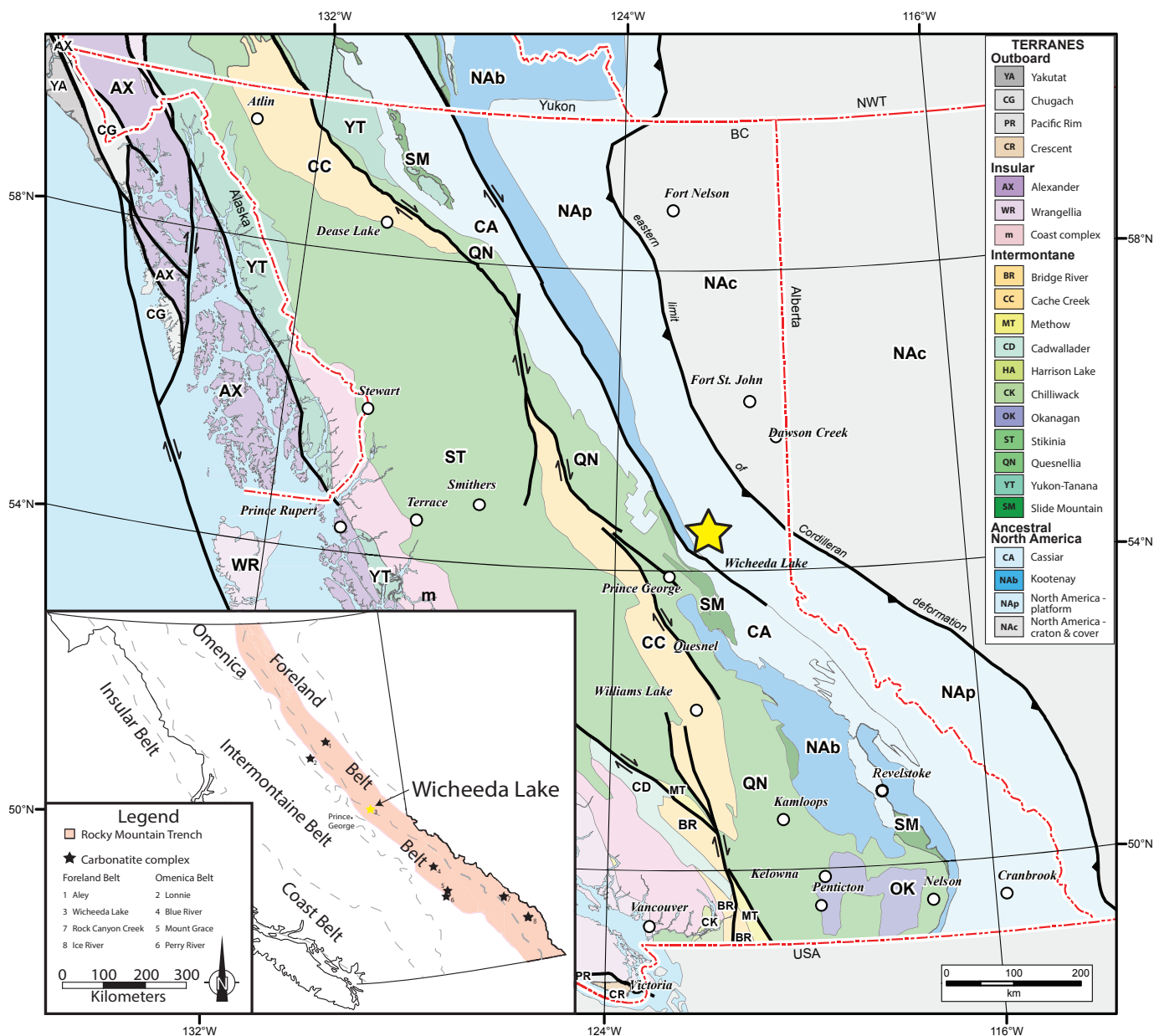


Fig. 1. Terrane assemblages and major tectonic features of Western Canada, with the Wicheeda Lake carbonatite highlighted by the yellow star. Inset: Distribution of major tectonic belts (dashed lines) and the Wicheeda carbonatite. The British Columbia alkaline Province is outlined in pink. From Colpron and Nelson (2011). Inset from Pell (1994).

2. Deposit geology

The Wicheeda complex is a dolomite and calcite carbonatite intrusion which, based on sparse outcrop and drill hole data, appears to be semi-circular in plan view (Fig. 2). On its western flank, the carbonatite is in fault contact with unaltered Kechika Group metasedimentary rocks. East of the fault, the carbonatite is surrounded by Kechika Group argillaceous limestone (Betmanis, 1987), which has been altered to potassic and sodic fenite (Fig. 2). Two outcrops of carbonatite and one of fine-grained felsic igneous rock lie to the east of the main carbonatite intrusion (Fig. 2).

The following descriptions are based on field mapping and petrographic examination using a combination of transmitted and reflected light microscopy, energy-dispersive X-ray spectroscopy (EDS)-assisted scanning electron microscopy, and cathodoluminescence.

2.1. Carbonatite

Dolomitic carbonatite occurs in the central part of the main intrusion and as an isolated outcrop ~ 150 m northeast of the main intrusion (Fig. 2). On the northeast margin of the complex, dolomite carbonatite passes gradually into a fine-grained calcite carbonatite. Calcite carbonatite is also exposed

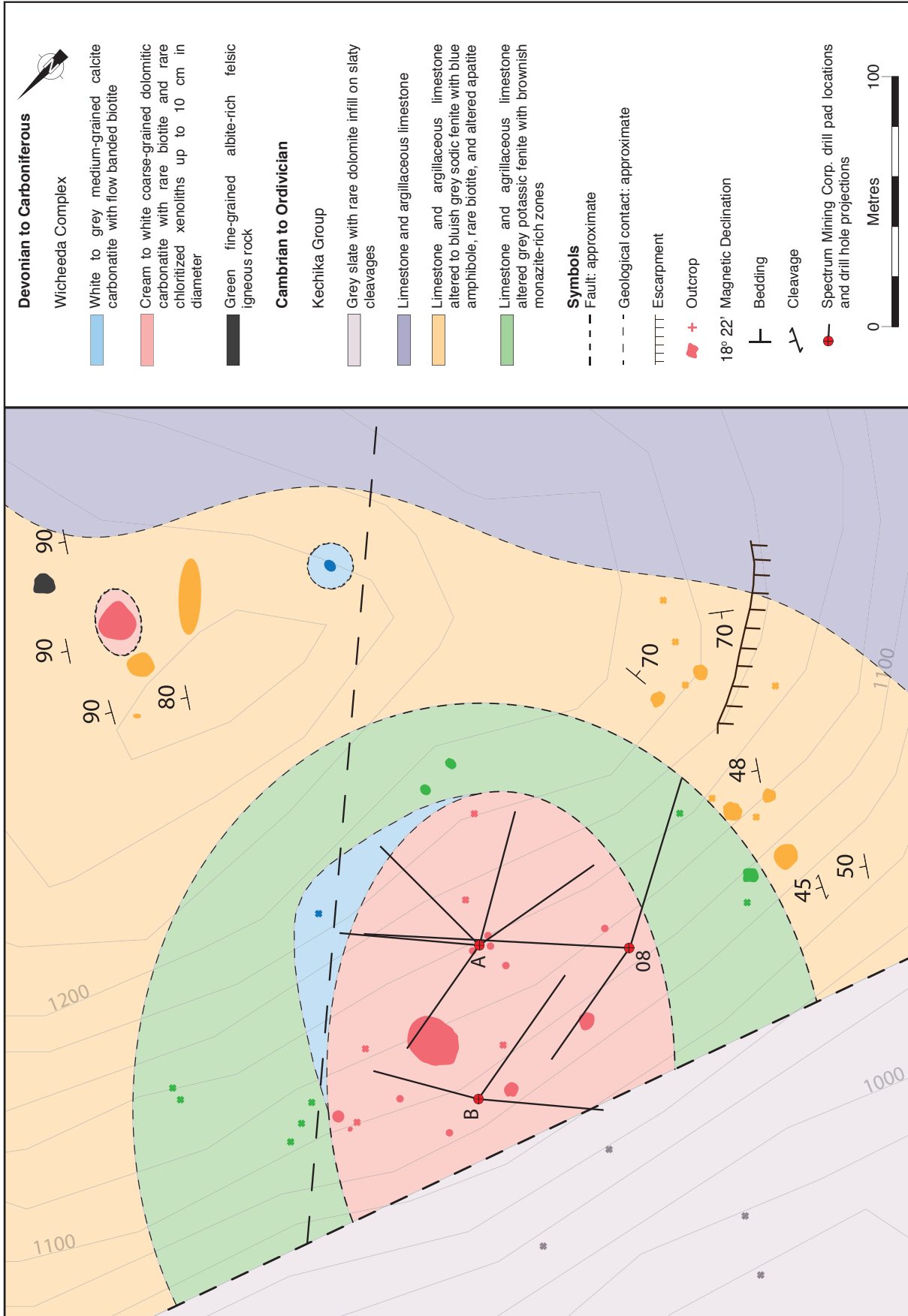


Fig. 2. Geological map of the Wichheeda carbonatite (at 54.315N, 122.051W). The location and geometry of the intrusion in relation to faults is based on fieldwork conducted in the summer of 2013.

in a single outcrop east of the main intrusion (Fig. 2).

In most outcrops, the dolomitic carbonatite is heavily oxidized dark orange or brown; where fresh, it is white to cream (Fig. 3a). It consists mainly of large euhedral dolomite crystals (70-80 vol.%) up to 2 cm in diameter accompanied by vein and vug-filling K-feldspar (5-15 vol%), dark micas (5-15 vol. %), pyrite (5 vol.%), hematite (2-5 vol.%), calcite (5 vol.%), and REE-fluorocarbonates (3-5 vol.%) including bastnäsite-(Ce) (CeCO_3F), parisite-(Ce) ($\text{CaCe}_2(\text{CO}_3)_3\text{F}_2$), synchysite-(Ce) ($\text{CaCe}(\text{CO}_3)_2\text{F}$), burbankite-(Ce) ($(\text{Na,Ca})_3(\text{Sr,Ba,Ce})_3(\text{CO}_3)_5$; 1 vol.%), and euhedral monazite-(Ce) (CePO_4 ; 1-3 vol.%). Three varieties of dolomite have been recognized. The first two comprise a relatively clear, coarse-grained, inclusion-poor variety (Dol I) and a dusty, micro-fluid inclusion-rich variety (Dol II; Figs. 3b, c). The third variety is a strongly zoned, cavity infill dolomite (Dol III; Fig. 3d). Biotite (< 2 mm flakes) and pyrite (rare euhedral cubes, < 3 mm) are disseminated in the dolomite carbonatite. Hematite (2-5 vol.%) occurs as weakly formed selvages to cleavages and veins. Calcite crosscuts the dolomite as veinlets up to 5 mm wide. Accessory rutile and molybdenite are observed as inclusions and clusters of grains in cobble- to boulder-sized chloritized xenoliths and are found within 10 metres of the contact with the fenitized sedimentary rocks. Bastnäsite-(Ce) occurs as a vug-filling phase with fan-like intergrowths of parisite-(Ce) and synchysite-(Ce) (Figs. 3b, e), which nucleates along fractured dolomite grains. Monazite-(Ce) is found as small, isolated, lath-like crystals or aggregates of crystals in vugs or veins (Fig. 3c) and rarely as fine-grained inclusions in bastnäsite-(Ce). Burbankite-(Ce) occurs in veinlets and very fine-grained inclusions in bastnäsite-(Ce). Niobian rutile ($(\text{Ti,Nb})\text{O}_2$) (1 vol.%) forms subhedral grains included in biotite and K-feldspar.

The calcite carbonatite comprises medium-grained, equigranular, fluid inclusion-rich calcite (85-90 vol.%; Fig. 4a) with minor biotite (5-15 vol.%), albite (5-10 vol.%), aegirine (2-3 vol.%), pyrochlore (1 vol.%), cubic pyrite (1-2 vol.%), and trace apatite. Flow banding is evident locally from alternating millimetre-thick layers containing 10 to 15 vol.% of biotite crystals up to 200 μm in diameter and thicker (2 – 5 mm) calcite-rich layers (Fig. 4a). The albite is very fine-grained, with crystals generally < 100 μm long. Commonly, the crystals contain inclusions of small rounded calcite up to 4 μm in diameter (Fig. 4b). The aegirine forms small euhedral crystals up to 100 μm long and is encountered most commonly in calcite carbonatite near the contact with the dolomite carbonatite. Trace pyrochlore occurs as brownish euhedral grains up to 200 μm in diameter (Fig. 4c). Pyrite cubes, typically > 100 μm in diameter (1-2 vol.%) and zoisite locally occur in cavities (Fig. 4c). The isolated calcite carbonatite to the east is very similar to that in the northeastern part of the main intrusion.

2.2. Kechika Group metasedimentary rocks

The Kechika Group metasedimentary rocks exposed west of the NE-SW trending fault comprise weakly foliated grey slates with a well-developed cleavage and fractures infilled by

dolomite. The rocks surrounding the study area to the north, east, and south (east of the NE-SW trending fault), are thickly bedded, steeply dipping limestone and argillaceous limestone (Fig. 2; Betmanis, 1987). In the study area they have been altered to fenite. Bedding is preserved in the fenite; the strike ranges from 320 to 350° and the dip from 45 to 90° (Fig. 2).

2.3. Fenite

Adjacent to the main carbonatite intrusion, except on its western, fault-bounded side, the Kechika metasedimentary rocks have been altered to potassic fenite for distances varying from 40 m to more than 75 m from the intrusion (Fig. 2). Beyond this, to the north, east, and south, the potassic fenites pass gradationally into sodic fenites that persist to the limits of the outcrop in the study area (Fig. 2). Northeast of the carbonatite, the contact between the potassic and sodic fenite is unconstrained because of a lack of outcrop.

The potassic fenite outcrops poorly and the following descriptions are based mainly on drill core. It varies in colour from pale beige (strongly altered) to pale grey (least altered) (Fig. 5a) and is composed mainly of fine-grained anhedral albite (20-30 vol.%) that has been extensively altered to K-feldspar (35-45 vol.%). The K-feldspar is generally found as small anhedral grains (up to 50 μm in diameter) containing rare albite inclusions (Fig. 5b). Calcite (15 vol.%) is interstitial to K-feldspar and albite, and is rimmed by dolomite (10 vol.%). Rutile (2-5 vol.%) occurs locally as large grain aggregates (Fig. 5b). Apatite (2-5 vol.%) forms anhedral fragmented grains up to 100 μm in diameter (Fig. 5c) and contains albite inclusions up to 10 μm in length. It is rarely altered to britholite-(Ce) ($(\text{Ce,Ca,Th,La,Nd})_3(\text{SiO}_4\text{PO}_4)_3(\text{OH,F})$), and contains elevated REE based on its blue to violet luminescence (e.g., Kempe and Götze, 1988). Monazite-(Ce) (2-3 vol.%) typically occurs as aggregates of small euhedral grains up to 20 μm in diameter. It is concentrated near the contacts between dolomite and K-feldspar crystals, and is frequently observed as a cavity-filling phase within the dolomite (Fig. 5c). Burbankite-(Ce) is found most commonly in thin veinlets in the potassic fenite and at the contact with the sodic fenite.

The sodic fenite consists mainly of albite (25-35 vol.%), calcite (25-35 vol.%), and riebeckite (15-20 vol. %). Sedimentary layering locally survived fenitization, and is preserved as alternating albite- and calcite-rich laminations (Fig. 6a). Albitic laminations consist of fine-grained subhedral albite laths up to 0.1 mm in length and subordinate, very fine-grained anhedral calcite. The albite is accompanied by fine-grained pyrite (oxidized in surface exposures). The calcite laminations are coarser-grained, with individual crystals ranging up to 0.8 mm in diameter. Bluish-green riebeckite is present as corroded subhedral prisms up to 100 μm in length and rarely as acicular grains. Brown biotite (15-25 vol.%) occurs as fine-grained disseminated flakes, and dark, euhedral apatite grains up to 1 mm in diameter are present throughout the albite + calcite matrix and in veinlets with calcite (Fig. 6b). Commonly, chlorite rims the biotite grains in the veinlets (Fig. 6c). Fractures in the

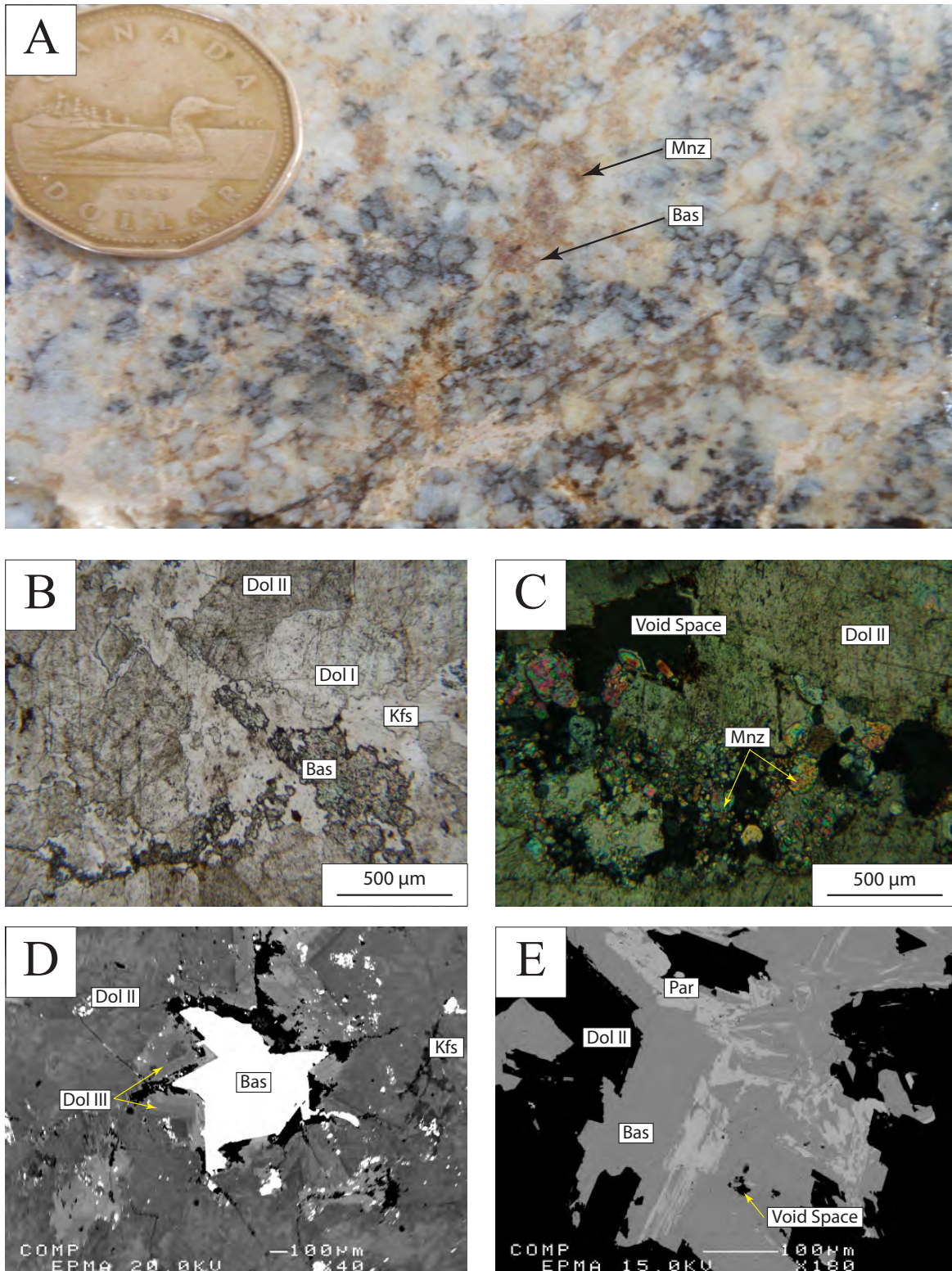


Fig. 3. **a)** Dolomite carbonatite showing brecciated dolomite with hematite (dark red) crackle texture overprinted by beige dolomite and fracture-filled brownish monazite-(Ce) (Mnz) and bastnäsite-(Ce) (Bas). **b)** Dolomite carbonatite in plane polarized light with clear Dol I and dusty Dol II dolomite and fractures infilled by K-feldspar (Kfs) and coarse bastnäsite-(Ce). **c)** Dolomite carbonatite under cross polars showing dusty dolomite Dol II and a fracture filled by K-feldspar and fine-grained monazite-(Ce). **d)** Backscatter electron image of dolomite carbonatite showing dusty dolomite with poorly defined grain boundaries Dol II and a strongly-zoned dolomite Dol III in a cavity infilled by bastnäsite-(Ce). **e)** Backscatter electron image showing a cavity in dolomite carbonatite infilled by syntaxial intergrowths of bastnäsite-(Ce) and parisite-(Ce) (Par).

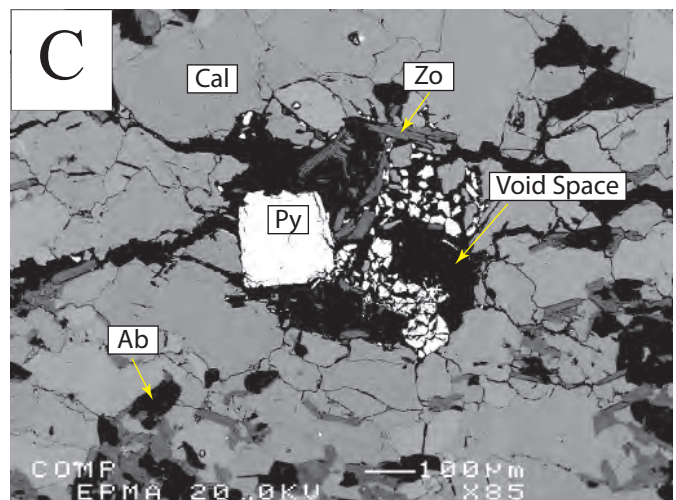
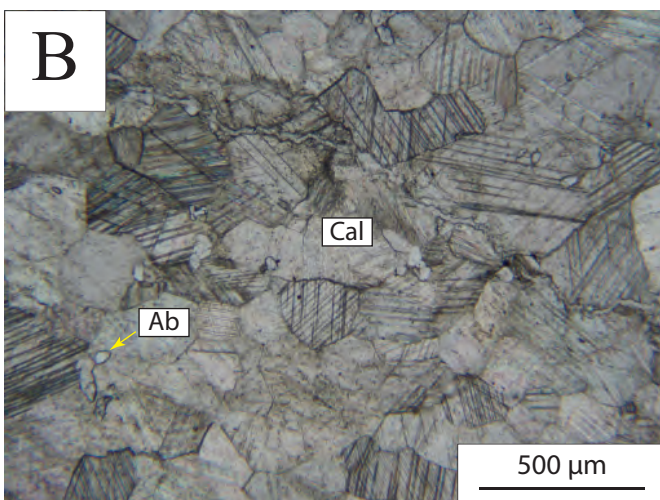
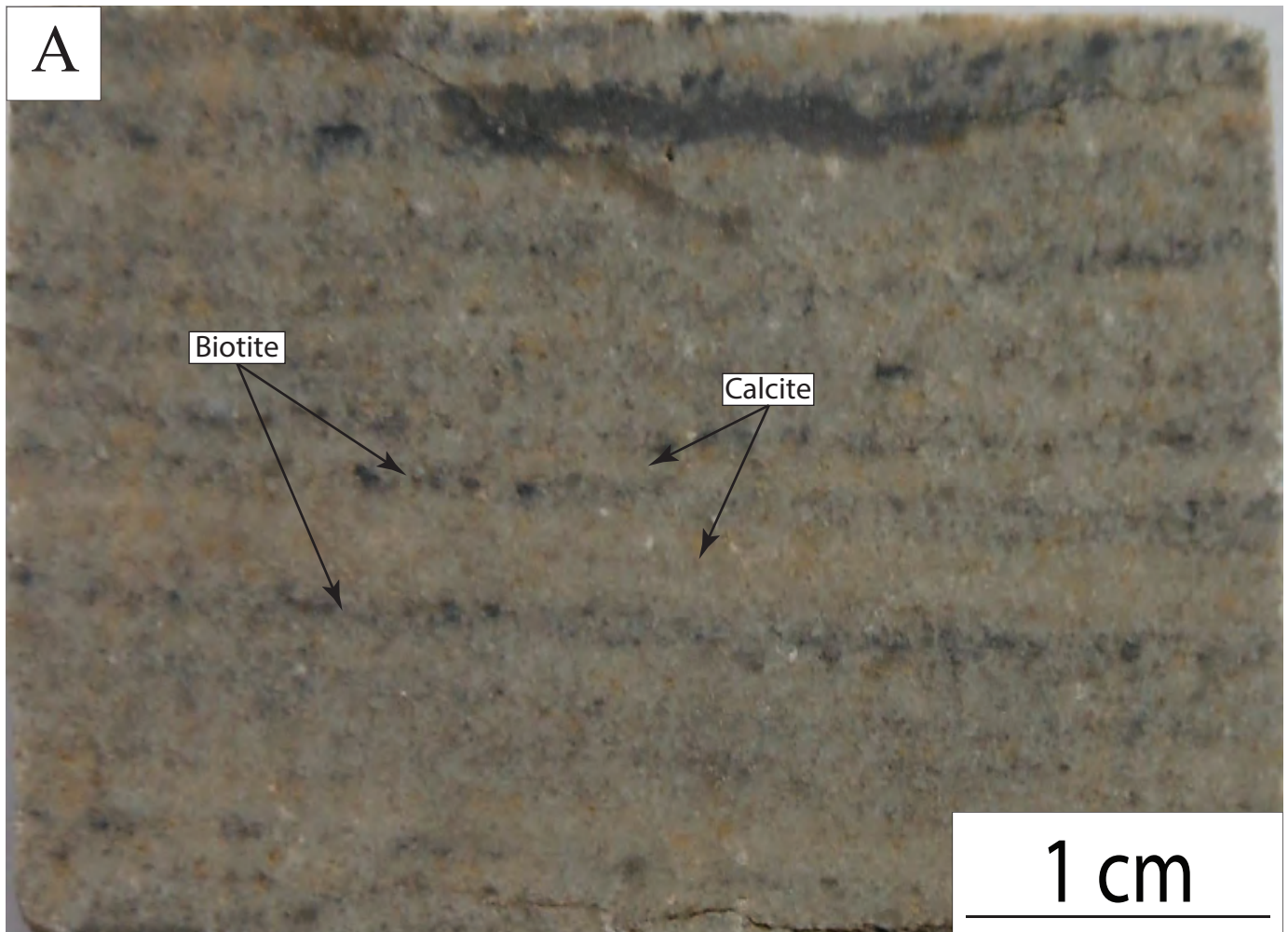


Fig. 4. Calcite carbonatite. **a)** Photograph of calcite carbonatite with alternating dark biotite-rich and white to pale grey calcite layers. **b)** Plane-polarized light image of fine-grained equigranular calcite (Cal) in calcite carbonatite accompanied by very small rare grains of albite (Ab). **c)** Backscattered electron image showing fractured calcite carbonatite containing a vug partially filled by pyrite (py), zoisite (Zo) and albite; albite is also disseminated in the matrix of the carbonatite.

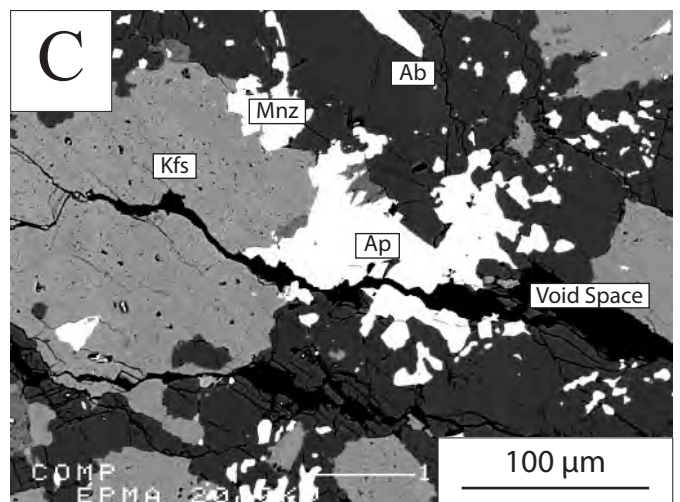
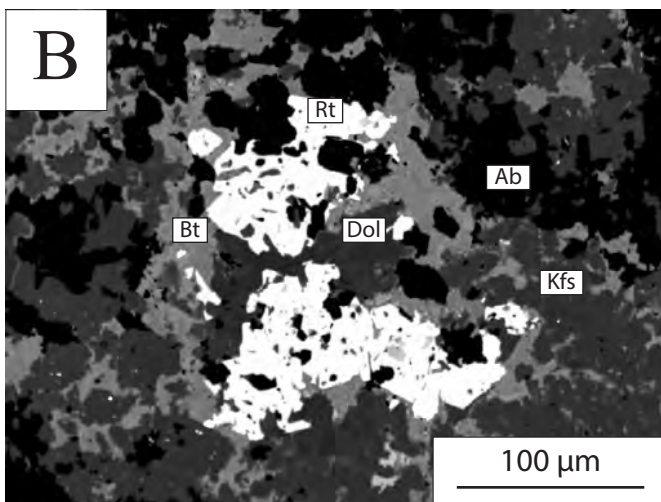
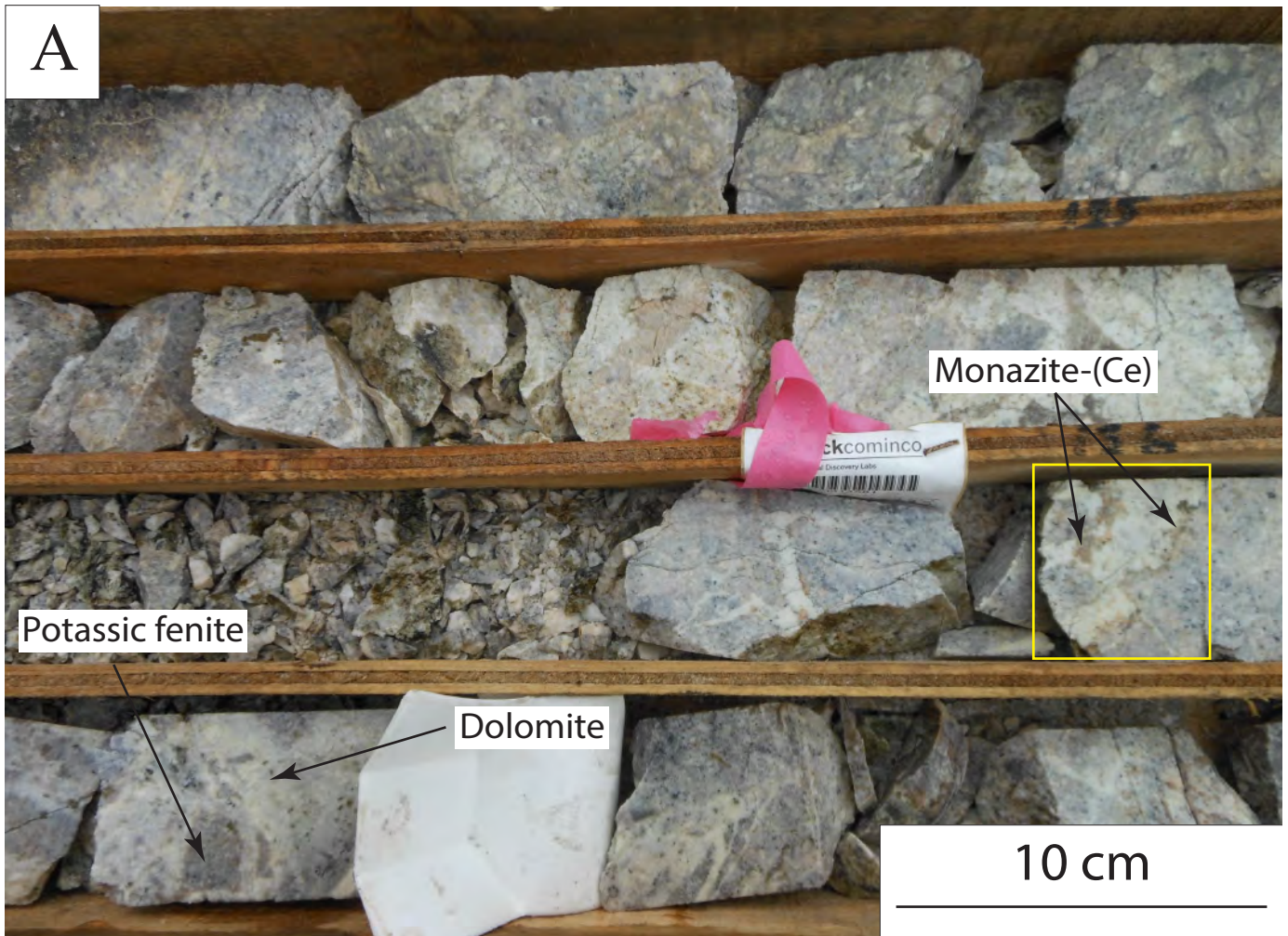


Fig. 5. Potassic fenite. **a)** Intensely altered potassic fenite from drill hole WI-09-08 (~ 135 m depth) showing beige clots of monazite-(Ce) at the contact between the fenite and dolomite-filled fractures. **b)** Backscattered electron image of potassic fenite showing albite variably replaced by K-feldspar, biotite, rutile (Rt) and dolomite (Dol). **c)** Backscattered electron image of potassic fenite with apatite and monazite-(Ce) replacing albite and K-feldspar.

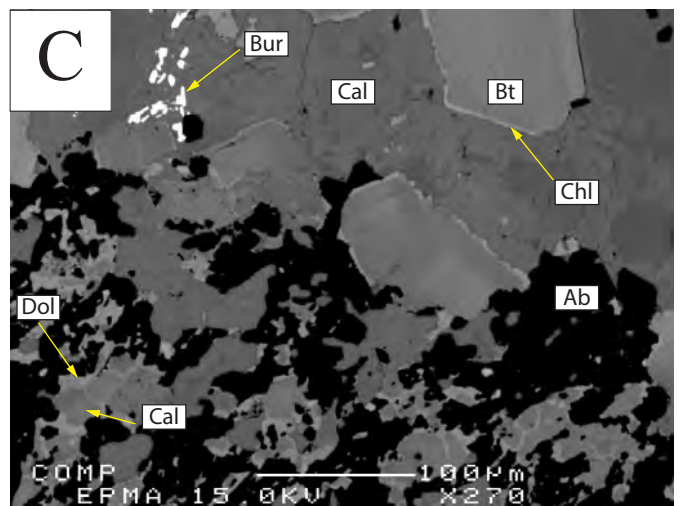
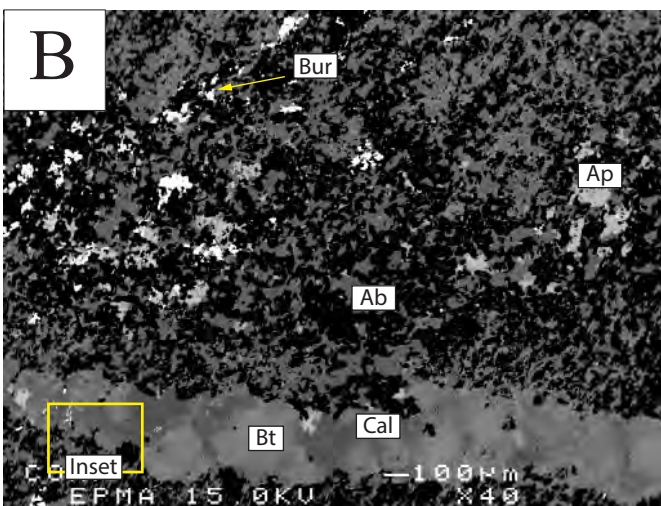


Fig. 6. Sodic fenite. **a)** Fractured sodic fenite from drill hole 08-W1-01 (180 m depth) showing relict sedimentary layering of the Kechika Group rocks, evident as alternating pale blue and pale green-grey bands. **b)** Backscattered electron image of sodic fenite with mottled albite and calcite and a crosscutting veinlet of calcite (Cal), biotite (Bt), and burbankite-(Ce) (Bur). **c)** Inset of **b)** showing a calcite+biotite vein with biotite rimmed by chlorite (Chl).

sodic fenite are frequently filled with dolomite (10 vol.%), siderite (5 vol.%), and locally burbankite-(Ce) (1 vol.%; Fig. 6b) near its contact with the potassic fenite. A lack of alignment of the secondary minerals described above suggests that sodic fenitization post-dated regional metamorphism.

3. Bulk Rock Geochemistry

Fourteen samples of the Wicheeda Lake carbonatite and associated fenite were analysed by ALS Laboratories in Vancouver for their bulk and trace element compositions. All samples were ground using a steel mill. The major element chemistry was determined using lithium metaborate fusion followed by Inductively Coupled Plasma Emission Spectrometry (ICPES). Loss on ignition (LOI) was determined after fusion. Total carbon and sulphur contents were determined using the LECO combustion method. The other trace elements were analyzed by Inductively Coupled Plasma Mass Spectrometry (ICPMS). The results are summarized in Table 1 and illustrated in Figs. 7- 9.

3.1. Carbonatites

Eight samples were analyzed from the dolomitic core of the main intrusion (Table 1). The main non-volatile components are CaO (25.8 wt.%), MgO (13.28 wt.%) and Fe₂O₃ (8.28 wt.%). ΣREE concentrations average 4.5 wt.% and range from 1.1 to 11.2 wt.%. There are also minor concentrations of P₂O₅ (0.89 wt.%), SrO (0.13 wt.%), BaO (0.81 wt.%), S (0.34 wt.%) and F (0.5 wt.%). The concentration of Nb averages 88 ppm and ranges from 4 ppm to 219 ppm. Concentrations of TiO₂ are below the detection limit for all of the samples.

One sample of the calcite carbonatite was analyzed (Table 1). It contains more CaO (44.9 wt.%), less MgO (2.24 wt.%), and less Fe₂O₃ (4.22 wt.%) than the dolomite carbonatite. The contents of SrO (1.59 wt.%) and P₂O₅ (2.46 wt.%) are very much higher, and the BaO content (0.32 wt.%) lower than the dolomite carbonatite. The calcite carbonatite contains an order of magnitude lower ΣREE (0.4 wt.%) than the dolomite carbonatite and virtually no fluorine, but is very enriched in Nb (2500 ppm).

The carbonatites were classified using the carbonatite classification diagram of Gittins and Harmer (1997). Based on its content of Ca, Mg, Fe, and Mn, the marginal carbonatite sample classifies as a calcio-carbonatite. The eight samples collected from the core of the intrusion classify as magnesio-carbonatite, although one of these samples plots on the border of the magnesio-carbonatite and ferruginous calcio-carbonatite fields (Fig. 7).

3.2. Fenites

The potassic fenite contains an average of 27.2 wt.% SiO₂, 7.2 wt.% Al₂O₃, 8.7 wt.% Fe₂O₃, 9.0 wt.% MgO, 2.92 wt.% K₂O and 0.5 wt.% Na₂O (Table 1). It has a high content of ΣREE (0.51 wt.%), Nb (1140 ppm) and P₂O₅ (0.76 wt.%) relative to the sodic fenite, but the lowest BaO (0.07 wt.%) and SrO (0.1 wt.%) contents of any of the rocks in the study area. It also

contains 0.52 wt.% S and has an F content below the detection limit.

The single sodic fenite sample (Table 1) contains more SiO₂ (37 wt.%), and Na₂O (5.5 wt.%) than the potassic fenite, less Fe₂O₃ (6.2 wt.%), and has a relatively low K₂O content (0.82 wt.%). It also contains more SrO (0.48 wt.%) and BaO (0.16 wt.%) than the potassic fenite, but a lower content of P₂O₅ (0.42 wt.%) and a very much lower content of S (0.02 wt.%). The ΣREE (0.09 wt.%) and Nb (29 ppm) contents are likewise very low and the F content below the detection limit.

The differences in the Na₂O and K₂O contents of the potassic and sodic fenites confirm the classification of the two fenite types (Fig. 8), which was inferred initially from the differences in their mineralogy. In combination with differences in the contents of SiO₂, Al₂O₃, Fe₂O₃ and Nb, this also suggests that the fluids responsible for the two types of fenite likely had different sources (see below).

4. REE Distribution

Chondrite-normalized REE profiles for the Wicheeda carbonatites and fenites are LREE-enriched and lack a europium anomaly (Fig. 9). The profiles of the carbonatites, and the potassic and sodic fenite are similar, although the REE content of the dolomite carbonatite is significantly higher than those of the other rocks types (Fig. 9). The dolomite carbonatite is highly enriched in LREE (La/Lu = 4314), whereas the calcite carbonatite has a much lower degree of LREE enrichment (La/Lu = 204) and is less enriched in the REE than all except one of the fenite samples. The potassic fenite samples have REE contents comparable to or slightly greater than the calcite carbonatite. They are strongly enriched in the HREE relative to the calcite carbonatite (Fig. 9) with La/Lu values of 1209 and 1288; the Yb and Lu contents of the most REE-enriched fenite are comparable to those of the most REE-enriched dolomite carbonatite. The sodic fenite sample is the least LREE enriched of all the samples analyzed and has a La/Lu ratios of 46.

4.1. Element correlations

As discussed above, the REE mineralization at Wicheeda is largely restricted to the dolomite carbonatite. A correlation coefficient matrix was generated for the dolomite carbonatite to evaluate relationships of cerium (as a representative of the light REE) with elements in host rocks that may have influenced its concentration (Table 2). The coefficients for Ce-F, Ce-Ba, and Ce-P are 0.96, 0.39, and -0.30, respectively. The high correlation between Ce and F is consistent with the observation that fluorocarbonates such as bastnäsite-(Ce) (CeCO₃F) are an important host for the REE and that there are negligible proportions of other fluorine-bearing minerals, such as fluorite or fluorapatite. By contrast, although the correlation between Ce and Ba can be explained, in part, by the occurrence of burbankite (Na,Ca)₃(Sr, Ba, Ce)₃(CO₃)₅, its low value suggests the presence of other barium-bearing minerals or elevated concentrations of Ba in carbonate minerals or K-feldspar. Preliminary microscopic examination (optical and

Table 1. Bulk rock compositions of dolomite and calcite carbonatites, and sodic and potassic fenites, Wicheeda Lake. bdl - below detection limit. Σ RREE – sum of rare earth elements and yttrium.

%	Detection Limit	Dolomite Carbonatite										Calcite Carbonatite WI-13-50	Potassic Fenite		Sodic Fenite WI-13-55
		WI-11-02	WI-11-03	WI-11-07	WI-11-09	WI-11-11	WI-11-12	WI-13-49	WI-13-62	WI-13-57	WI-13-63				
SiO ₂	0.01	4.45	4.22	3.45	2	1.05	5.42	3.55	1.48	6.33	20	34.4	37		
Al ₂ O ₃	0.01	1.41	1.16	0.96	0.53	0.28	1.56	0.31	0.28	1.78	5.86	8.49	6.46		
Fe ₂ O ₃	0.01	8.23	8.08	6.31	6.91	9.5	6.54	10.65	10	4.22	7.74	9.62	6.2		
CaO	0.01	26.2	23.8	23.3	21	27.6	27.1	27.9	29.7	44.9	20.8	14.15	22.4		
MgO	0.01	13.55	13.1	13.05	13.8	12.3	14.25	12.8	13.4	2.24	8.55	9.36	3.22		
Na ₂ O	0.01	0.37	0.69	0.66	0.26	0.14	0.88	0.18	0.04	0.44	0.37	0.62	5.45		
K ₂ O	0.01	0.47	0.1	bdl	0.04	bdl	0.04	0.02	0.13	0.7	4.44	1.42	0.82		
Cr ₂ O ₃	0.01	bdl	bdl	bdl	bdl	bdl	bdl	bdl	bdl	bdl	bdl	bdl	bdl		
TiO ₂	0.01	bdl	bdl	bdl	bdl	bdl	bdl	bdl	bdl	0.22	0.2	0.48	0.27		
MnO	0.01	1.24	1.07	0.82	0.36	1.69	0.87	1.91	1.9	0.83	1.36	0.57	0.51		
P ₂ O ₅	0.01	1.38	0.21	1.39	0.04	1.7	1.44	0.87	0.01	2.46	1.34	0.18	0.42		
SrO	0.01	0.06	0.17	0.2	0.06	0.13	0.05	0.11	0.09	1.59	0.13	0.06	0.48		
BaO	0.01	0.17	0.61	0.81	0.17	0.04	bdl	0.03	0.03	0.32	0.07	bdl	0.16		
LOI	0.01	38.8	36.8	37.6	35.2	39.5	39.2	40.1	42.3	32.4	27.7	18.75	17.5		
Total		96.33	90.02	88.56	80.22	93.93	97.36	98.43	99.37	98.43	98.56	98.14	100.89		
C	0.01	10.35	10.95	10.7	10.55	11.3	11	12.2	12.9	9.64	8.26	5.21	4.91		
S	0.01	0.04	0.88	0.26	1.39	0.08	0.03	0.03	0.03	0.61	0.05	0.98	0.02		
F	0.01	0.09	0.7	0.61	1.45	0.02	0.07	bdl	bdl	bdl	bdl	bdl	bdl		
ppm															
Nb	0.2	153	62.2	27.2	191.5	33.7	4	13.6	219	2500	559	1720	29.3		
Th	0.05	301	898	1000	1000	422	252	454	217	54.7	175.5	82.8	33.6		
U	0.05	2.78	2.35	0.98	2.02	0.5	0.34	0.53	2.72	27.7	7.73	24	0.4		
Zr	2	bdl	bdl	bdl	bdl	bdl	bdl	bdl	bdl	108	bdl	3	211		
La	0.5	11000	22700	28300	40500	11100	6980	5720	3650	1105	2110	1165	229		
Ce	0.5	14500	27900	37000	53200	15300	8620	9000	5030	2040	3030	1685	402		
Pr	0.03	1100	2100	2800	4300	1100	844	820	419	177.5	261	147.5	37.1		
Nd	0.1	3340	6340	8710	11900	3670	2460	2520	1225	522	796	441	115.5		
Sm	0.03	311	450	682	900	334	265	281	127	55.4	107.5	55.1	15.95		
Eu	0.03	88.4	86.1	143.5	178	86	71.9	58.6	30.2	14.85	32.6	15.05	4.22		
Gd	0.05	162	175.5	280	390	164.5	145.5	121.5	58.7	27.7	70.6	30.9	10.7		
Tb	0.01	16.6	13.65	21.4	27.2	15.35	13.55	9.3	4.64	3.21	7.9	3.52	1.44		
Dy	0.05	62.5	43	66.6	84.4	53.9	50.5	24.7	12.65	14.05	28.9	13.15	7.64		
Ho	0.01	7.2	4.79	7.06	9.08	6.08	6.26	2.45	1.18	2.34	3.45	1.56	1.45		
Er	0.03	11.15	6.79	9.12	12.05	9.26	10.4	3.76	1.62	5.73	5.42	2.52	3.93		
Tm	0.01	0.9	0.54	0.72	0.9	0.79	0.93	0.29	0.11	0.65	0.4	0.2	0.52		
Yb	0.03	3.79	2.73	3.64	4.1	3.79	4.19	1.51	0.63	4.19	1.63	1.03	3.53		
Lu	0.01	0.41	0.34	0.47	0.53	0.47	0.49	0.24	0.09	0.56	0.17	0.1	0.52		
Y	0.5	130	102	143	190	117	136	53.9	24.4	62.5	66.5	31.2	38.5		
Σ RREE		30734	59925	78168	111696	31961	19609	18617	10585	4036	6522	3593	872		

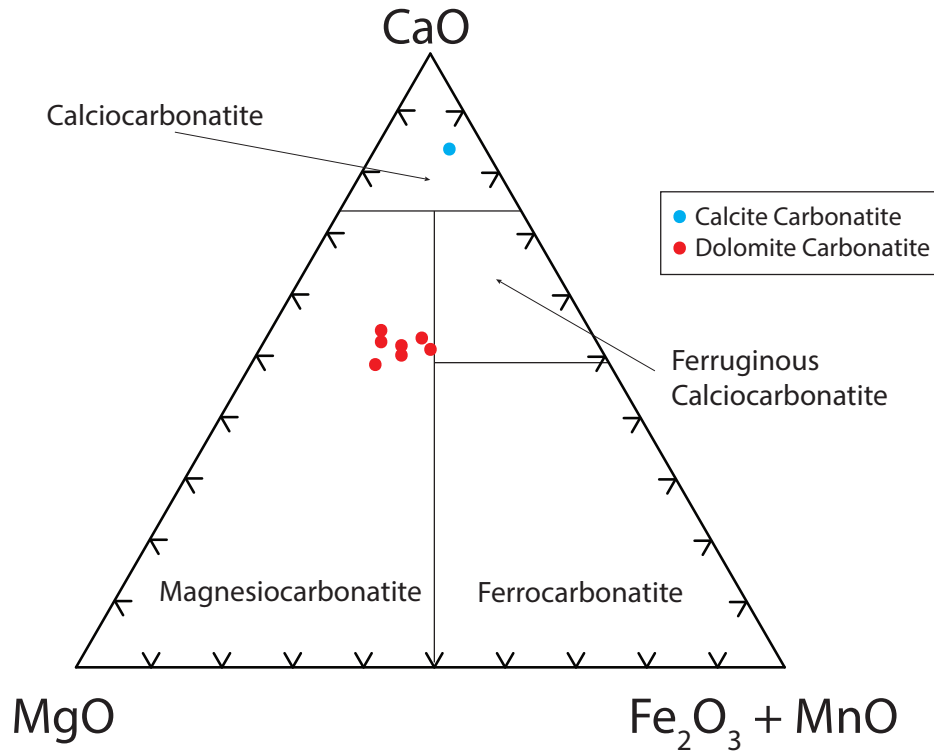


Fig. 7. Compositions of the carbonatite rocks of the Wicheeda area on the classification diagram of Gittins and Harmer (1997).

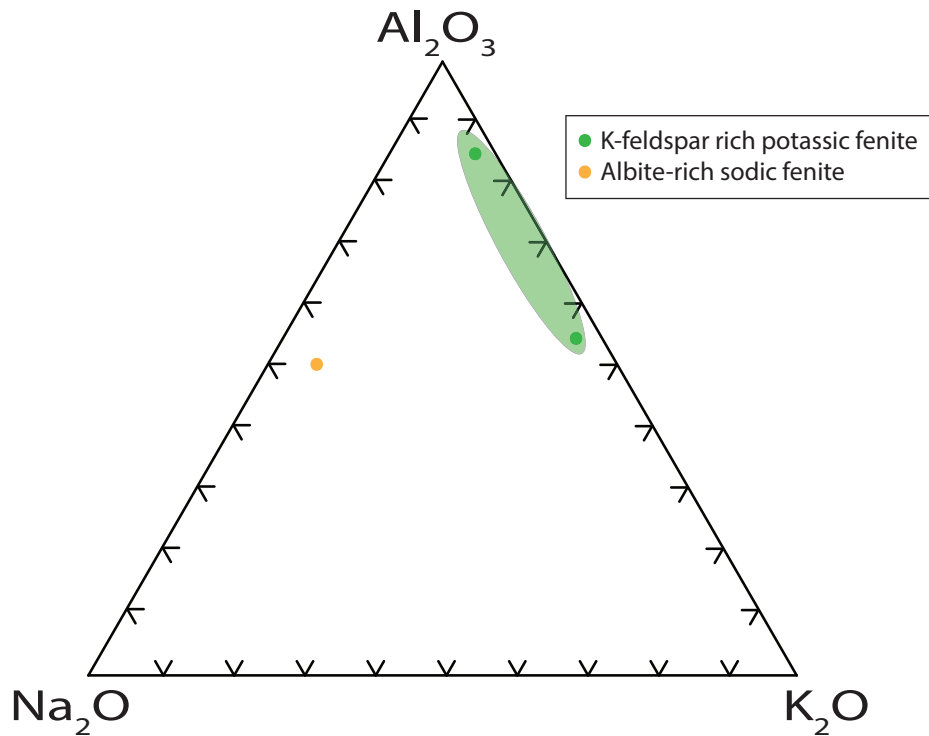


Fig. 8. Al_2O_3 - Na_2O - K_2O classification diagram for Kechika Group rocks altered to albite- (orange) and K-feldspar-rich (green) fenites or sodic and potassic fenites, respectively.

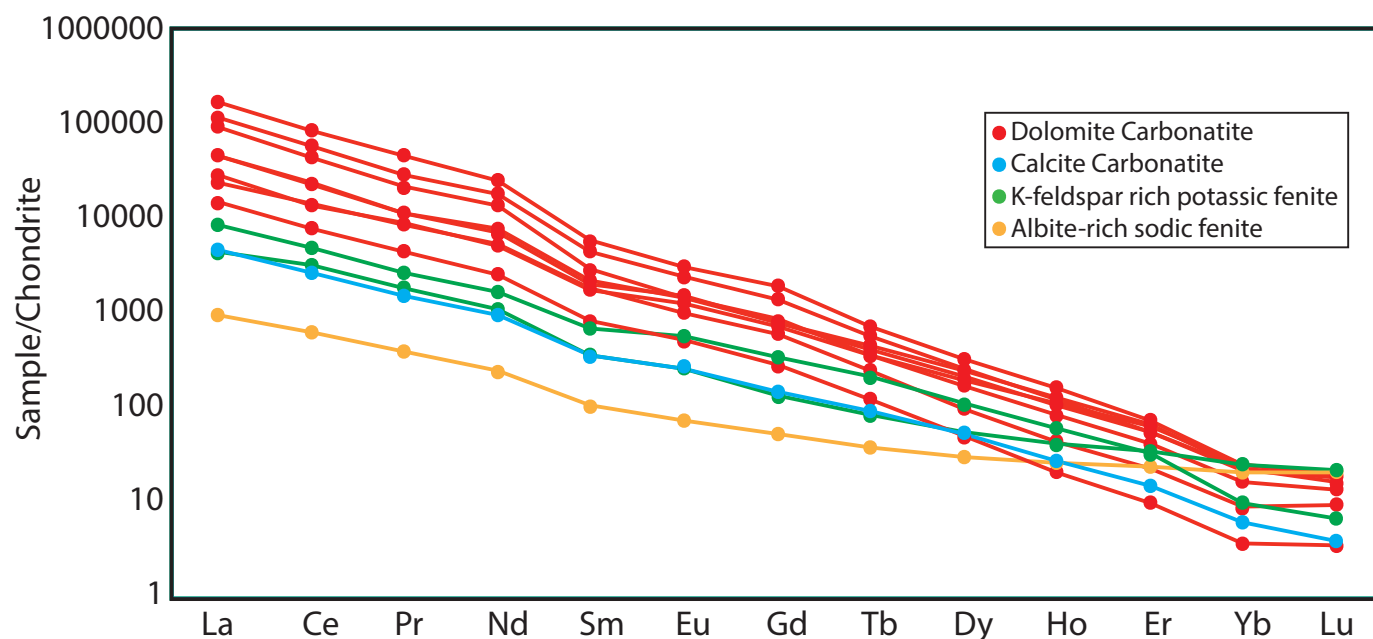


Fig. 9. Chondrite-normalized REE profiles of Wicheeda carbonatites and fenites. The chondrite values were taken from McDonough and Sun (1995).

Table 2. Correlation matrix of selected elements and oxides for dolomite carbonatite samples from the main intrusion. Data from bulk rock geochemistry.

	Ba	Ce	F	K ₂ O	Lu	Nb	Sm	P ₂ O ₅	Sr	Y	Yb
Ba	1										
Ce	0.39	1									
F	0.28	0.96	1								
K ₂ O	-0.06	-0.22	-0.21	1							
Lu	0.14	0.58	0.47	-0.11	1						
Nb	-0.29	0.19	0.30	0.46	-0.32	1					
Sm	0.36	0.99	0.93	-0.27	0.64	0.10	1				
P ₂ O ₅	0.06	-0.30	-0.50	0.08	0.48	-0.65	-0.20	1			
Sr	0.84	0.24	0.09	-0.38	-0.04	-0.43	0.21	0.09	1		
Y	0.16	0.75	0.67	-0.01	0.95	-0.06	0.79	0.24	-0.11	1	
Yb	0.12	0.48	0.38	0.05	0.98	-0.26	0.54	0.52	-0.12	0.93	1

EDS-assisted scanning electron microscopy), however, has not revealed the presence of other Ba-bearing minerals, e.g., barite, and K-feldspar, and K-feldspar has not yet been analyzed for its Ba content. The relatively poor Ce-Ba correlation remains unexplained.

As inclusions of monazite-(Ce) were observed in the dolomite carbonatite, we expected a weak positive correlation of Ce with P. Instead, the correlation is negative. We tentatively conclude that the signal of monazite-(Ce) was swamped by apatite (another phosphate mineral, which is found in minor proportions in the carbonatite) and that the apatite contains relatively little REE (this latter conclusion remains to be tested).

5. Discussion

Outcrop and drill core observations indicate that both the dolomite and calcite carbonatites and the host Kechika Group

metasedimentary rocks were strongly altered by hydrothermal fluids. The host rocks were altered to potassic fenite surrounding the carbonatite (40 – 75 m away) and sodic fenite to the extent of the outcrop in the mapped area; the distribution of the sodic fenite is poorly constrained.

The sodic fenite, which is represented mainly by albitization, is interpreted to be the product of alteration by formational waters heated by the carbonatite. This is supported by the observation that fluids, which are initially in equilibrium with two alkali feldspars (likely the case for formational waters in contact with siltstone), will move into the stability field of albite on being heated (Lagache and Weisbrod, 1977). Using the same line of reasoning, we interpret the potassic fenite (mainly K-feldspar) to be the product of saline aqueous fluids released by the carbonatite magma (e.g., Williams-Jones and Palmer, 2002). As these fluids would have followed a cooling

path after their exsolution, their physicochemical conditions would have evolved to the field of K-feldspar stability (Lagache and Weisbrod, 1977). Although, we do not know if these fluids were initially in equilibrium with two feldspars (the dolomite carbonatite contains primary K-feldspar but not albite) this is not important. The key observation is that whether or not they were initially in equilibrium with K-feldspar, they would have evolved towards its field of stability (the petrographic evidence suggests that they initiated in equilibrium with K-feldspar).

The rare earth mineralization is dominated by REE-fluorocarbonates accompanied by burbankite, cebaite-(Ce), and monazite-(Ce) in veinlets and vugs and as disseminations in the carbonatite and burbankite in veinlets in the potassic fenite and immediately adjacent sodic fenite. This shows that the mineralization is predominantly hydrothermal in origin. We propose a preliminary model in which the carbonatite magma exsolved a fluid, which fenitized the host metasediments near the intrusion to potassic fenite and heated formational water distal to the intrusion, altering the metasedimentary rocks to sodic fenite. The REE were concentrated by magmatic hydrothermal fluids, which partially dissolved the carbonatite, altering Dol I to Dol II, and led to deposition of compositionally zoned dolomite (Dol III) and later bastnäsite-(Ce) and monazite-(Ce) in veins and vugs in response to cooling and an increase in pH. As REE-fluoride mineral solubility is very low, except under extremely acidic conditions, it is proposed that REE-chloride complexes preferentially transported the REEs (Williams-Jones et al., 2012). There is the possibility that the REEs were transported as sulphate complexes (Migdisov and Williams-Jones, 2008), although this seems less likely given that sulphate minerals are rare to absent in the deposit. Like REE fluoride, REE-phosphate solubility is low, precluding the transport of elements like cerium as phosphate complexes. Instead, we consider that fluoride and phosphate acted as depositional ligands, promoting the concentration of the REE as fluorocarbonate minerals and monazite-(Ce).

6. Conclusions

The Wicheeda carbonatite is a high grade LREE deposit that was subjected to extensive alteration by magmatic fluids, and its intrusion was accompanied by pervasive fenitization of the wall rock to proximal potassic fenite and distal sodic fenite. Potassic fenitization was the product of cooling magmatic hydrothermal fluids and sodic fenitization the product of formational waters heated by the intrusion. The REE were concentrated by magmatic hydrothermal fluids, which deposited them dominantly as fluorocarbonate minerals in veinlets and vugs in the carbonatite, and to a much lesser extent as monazite-(Ce) in the potassic fenites, due to a combination of cooling and pH increase. Niobium is enriched in the calcite carbonatite in the form of pyrochlore, and is found rarely as hydrothermal niobian rutile in the dolomite carbonatite. In summary, the REE and associated HFSE mineralization in the Wicheeda deposit is exclusively hydrothermal in origin.

Acknowledgments

The authors are grateful to courtesies extended by Chris Graf. We also thank Spectrum Mining Corporation for permitting access to the property and facilities for logging the core, and Bob Lane (Plateau Minerals Corp.) for sharing his knowledge of the geology of the Wicheeda deposit. Duncan Mackay provided valuable assistance in the field and observations of the mineralization. The project received funding and support from Targeted Geoscience Initiative 4 (2010-2015), a Natural Resources Canada program carried out under the auspices of the Geological Survey of Canada. The authors would also like to thank Pearce Luck and Lawrence Aspler (British Columbia Geological Survey) for their reviews, which helped improve the manuscript.

References cited

- Betmanis, A.I. 1987. Report on geological, geochemical and magnetometer surveys on the prince and George groups, cariboo mining division, British Columbia Ministry of Energy, Mines and Petroleum Resources, Assessment Report 15944.
- Colpron, M., and Nelson, J.L. 2011. A digital atlas of terranes for the northern Cordillera. British Columbia Ministry of Energy and Mines, British Columbia Geological Survey, GeoFile 2011-11, scale 1:10 000 000.
- Gittins, J., and Harmer, R.E. 1997. What is ferrocarnatite? A revised classification. *Journal of African Earth Sciences*, 25, 159-168.
- Lagache, M., and Weisbrod, A. 1977. The system: two alkali feldspars -KCl-NaCl-H₂O at moderate to high temperatures and low pressure. *Contributions to Mineralogy and Petrology*, 62, 77-101.
- Lane, B. 2009. Diamond drilling report on the Wicheeda property. Allnorth Consultants: prepared for Spectrum Mining Corp.
- Lane, B. 2010. Diamond drilling report on the Wicheeda property. Unpublished Report, Allnorth Consultants: prepared for Spectrum Mining Corp. 1-18.
- Mäder, U.K., and Greenwood, H.J. 1987. Carbonatites and related rocks of the prince and George claims, northern rocky mountains (93J,93I). In: *Geological Fieldwork 1987*, British Columbia Ministry of Energy, Mines and Petroleum Resources, British Columbia Geological Survey Paper 1988-1, 375-380.
- Migdisov, A.A., and Williams-Jones, A.E. 2008. A spectrophotometric study of Nd(III), Sm(III), and Er(III) complexation in sulfate-bearing solutions at elevated temperatures. *Geochimica and Cosmochimica Acta*, 72, 5291-5303.
- Millonig, L.J., Gerdes, A., and Groat, L.A. 2012. U-Th-Pb geochronology of meta-carbonatites and meta-alkaline rocks in the southern Canadian Cordillera: A geodynamic perspective. *Lithos*, 152, 202-217.
- McDonough, W.F., and Sun, S.-s., 1995. The composition of the Earth. *Chemical Geology*, 120, 223-253.
- Pell, J., 1994. Carbonatites, nepheline syenites, kimberlites and related rocks in British Columbia. British Columbia Ministry of Energy, Mines and Petroleum Resources, British Columbia Geological Survey, Bulletin 88, 11-14.
- Williams-Jones, A.E., and Palmer, D.A.S. 2008. The evolution of aqueous-carbonic fluids in the Amba Dongar carbonatite, India: implications for fenitisation. *Chemical Geology* 185, 283-301.
- Williams-Jones, A.E., Migdisov, A.A., and Samson, I.M., 2012. Hydrothermal mobilization of the rare earth elements – a Tale of “Ceria” and “Yttria”. *Elements*, 8, 355-360.